

HOW CAN MATERIAL JETTING SYSTEMS BE UPGRADED FOR MORE EFFICIENT MULTI-MATERIAL ADDITIVE MANUFACTURING?

M. Baumers, C. Tuck, P. Dickens, and R. Hague

Additive Manufacturing and 3D Printing Research Group (3DPRG),
Faculty of Engineering, University of Nottingham, Nottingham, NG7 2RD, UK

REVIEWED

Abstract

Multi-material Additive Manufacturing (AM) platforms are able to build up components from multiple materials in a single layer-by-layer process. It is expected that this capability will enable the manufacturing of functional structures within products, such as conductive tracks or optical pathways, resulting in radically novel products with unprecedented degrees of functional density.

An important variant of commercially available multi-material AM technology is material jetting, which is currently in commercial use for the manufacture of prototypes and design studies. This paper presents a detailed process model of build-time, energy consumption and production cost for the Stratasys Objet 260 Connex system, analyzing the contemporaneous deposition of two different types of photopolymers (Veroclear RGD810 and Tangoblack FLX973). By using this process model to anticipate the effects of various upgrades to the investigated system, such as a larger build volume and a higher deposition speed, this forward-looking paper explores pathways to enhancing the value proposition of such multi-material systems through incremental technology improvement.

Introduction

Since the innovation of processes capable of additively depositing build material in the early 1980s, the spectrum of applications for these technologies has extended (Bourell et al., 2009; Shellabear and Nyrhilä, 2004; Melchels, 2012). It now ranges from the fast manufacture of design studies and prototypes to the small and even medium series manufacture of specialist high-value end use products (Lipson, 2012; Wohlers, 2012). The adoption of AM by industry carries a number of strategic implications (Cotteleer and Joyce, 2014). Moreover, it has been suggested that the technology has the potential for significant product innovation in the future and may alter the structure of the manufacturing sector in general (Lipson, 2012).

Used synonymously with the label “3D Printing”, AM can be defined as a collection of technologies capable of “joining materials to make objects from 3D model data, usually layer upon layer, as opposed to subtractive manufacturing methodologies” (ASTM, 2012). Among AM technologies, special significance for potential product and manufacturing process innovation is attributed to processes that are capable of depositing multiple materials (Espalin et al., 2014; Diginova, 2014), allowing the embedding of functional structures to create radically novel products.

It is suggested that AM technology has two main advantages over other manufacturing processes (Tuck et al., 2008). Firstly, AM allows the manufacture of designs without many of the geometric constraints that apply to other techniques. Secondly, AM enables the manufacture of customized products in small and medium volumes at a relatively low average cost. The current state of AM technology, however, carries a set of generic process

limitations (Ruffo and Hague, 2007), acting as a barrier against the adoption of AM process in some applications:

- limited material selection and characteristics,
- low process productivity,
- low dimensional accuracy,
- rough surface finish,
- repeatability and quality issues,
- relatively high unit cost at medium and large volumes.

By constructing a detailed-analysis approach (see, for example, Di Angelo and Di Stefano, 2011) to AM process modelling, this paper assesses the build time, energy consumption and cost performance of a commercially available AM system capable of concurrently processing multiple materials, the Objet Connex 260 (Stratasys, 2014). Using a validated process model, this paper explores how the productivity, energy efficiency and cost performance of this system could hypothetically be improved by upgrading a selection of machine characteristics and performance dimensions.

The operating principle of multi-material jetting systems and the main components are described in Figure 1. Within an enclosed build volume, shown here with its cover open, photopolymer droplets are deposited by a print head (a) onto a build platform (b). Moving in the in the X / Y plane, the print head also incorporates a UV light source to initialize a polymerization reaction and a planarization mechanism to remove excess material. After finishing the deposition of material and UV exposure within a layer, the build platform indexes down by one increment in the Z direction and the deposition process for the next layer begins. Fresh build material is fed to the jetting head from multiple material cartridges (c), each one containing a separate build material. An additional material required for the deposition of sacrificial structures connecting parts to the build plate and to support overhangs is supplied from support material cartridges (d). The excess material removed during the build process by planarization is transferred into a waste container (e).

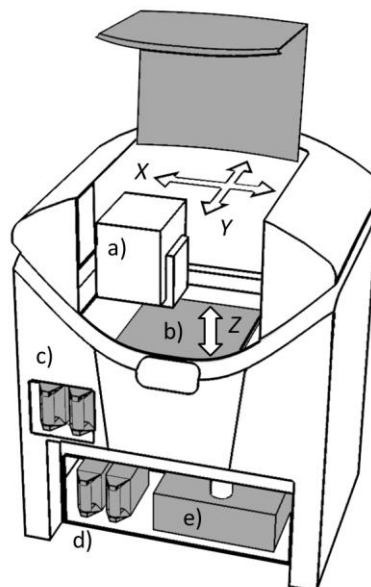


Figure 1: Main components of a material jetting system
Image source: own work

This build cycle is repeated layer-by-layer until the build operation is complete and the platform (b) can be removed by the machine operator. For additional details on the operating principle of such material jetting processes, see Gibson et al. (2010). Table 1 summarizes important characteristics of the investigated Stratasys Objet Connex 260 system.

Table 1: Stratasys Objet Connex 260 configuration, as investigated for this research

| System type | Objet Connex 260 |
|---------------------------------------|-----------------------------|
| Deposition type | Material jetting / printing |
| Nozzle type | Piezoelectric |
| Nominal build volume size (X / Y / Z) | 260 * 260 * 200 mm |
| Usable platform area (X / Y) | 250 * 250 mm |
| Primary (structural) build material | VeroClear RGD810 |
| Secondary (functional) build material | TangoBlack FLX973 |
| Support material | FullCure SUP705 |
| Layer thickness | 30 μ m |
| Process atmosphere | Normal ambient |
| Powder bed heating | none |
| Power supply | 240 V, single phase |
| Chiller on external power | no |
| Manufacturer reference | Stratasys (2014) |

Current AM processes based on material jetting are used primarily for model making, design visualizations and prototypes. As with other AM techniques, it is suggested that the technical capability and cost performance of such platforms must be enhanced to increase the application spectrum for material jetting technologies to include more true manufacturing applications, (Diginova, 2014). In particular, material jetting technology carries the promise of being an important enabler for multifunctional AM. The promise of multifunctionality is that it will allow the manufacture of a new generation of high value multifunctional products, featuring embedded functionalities and performing as integrated systems rather than passive components (Espalin, et al., 2014).

Showing how specific machine upgrades may result in overall cost performance improvements for material jetting systems, this paper pursues two objectives: firstly, it helps establish which directions for further technology developments may be especially worthwhile to realize material jetting systems which are better suited for true manufacturing applications. Secondly, it aims to provide orientation to the relative magnitude of the benefits resulting from such upgrades, in terms of deposition speed, energy consumption and financial cost.

Methodology

To approach the research objective, this paper builds a detailed-analysis process model of the Objet 260 Connex system. After collecting the required empirical data by evaluating a build experiment based on a dedicated test geometry (as done, for example, by Mognol et al., 2006), the data are inserted into an existing general purpose framework for the combined estimation of build time, energy consumption and cost (see Baumers et al., 2013). Following the validation of the process model by measuring its estimates against a real build experiment

based on parts drawn from a basket of three multi-material test specimens, the model is ready to be used to explore the effects of various upgrades to system capability.

Building a detailed process model

Generally, build time estimators form a suitable costing approach for capital-heavy production processes (see, for example, Atrill and McLaney, 1999). Thus, build time estimation provides the foundation for several AM production cost models (Alexander et al., 1998; Byun and Lee, 2006; Campbell et al., 2008). Moreover, it has been shown that some AM processes operate efficiently only where the available capacity is fully utilized (Ruffo et al., 2006; Baumers et al., 2011). This implies that to claim that an AM process is used at full capacity, it may be necessary to configure the build process to contain the maximum possible number of parts. For the automated filling of AM build volumes, workspace packing algorithms have been implemented (Wodziak et al., 1994; Nyaluke et al., 1996; Ikonen et al., 1997).

The process model developed for this paper is based on an adaptation of an existing general purpose framework combining an automated build volume packing technique with build time estimation (described in detail by Baumers et al., 2013). Implemented in C++ using the open source development environment Dev-C++ (v.4.9.9.2), the model is based on voxel approximations of part geometries, as proposed by Hur et al., (2001). To keep the implementation relatively concise, a number of simplifications were made. These include the following:

- to create a suitable build volume configuration, the model is based upon rough voxel representations of parts drawn from a basket of three multi-material demonstration components (with a resolution of 5 mm). This discretizes the problem of placing irregular and continuous geometries. As the main purpose of the voxel representations is to facilitate build volume packing, they do not contain information on the materials present in each voxel.
- In order to eliminate the possibility of anisotropic material properties and unpredictable part behavior, part rotation is constrained to the vertical axis. For further ease of implementation, the rotation of the test components is also limited to discrete 90° steps.
- On the Objet Connex 260, all parts must be connected to a removable build plate forming the build volume floor, as shown in Figure 1 (b). Therefore, the automated packing functionality considers only arrangements in which all parts are placed on the substrate, effectively limiting part movement to the X / Y plane.
- As the deposition regime for multiple photopolymer materials deposited by the Objet Connex 260 system is very similar, if not identical, the time estimation part of the proposed model is not designed to distinguish between different build materials.

To build the process model, the first step is to estimate build time, T_{Build} , which is obtained by combining data from a hierarchy of three elements of time consumption: (i) fixed time consumption per build operation, T_{Job} , including machine warm up, (ii) total Z-height-

dependent time consumption, obtained by multiplying the fixed time consumption per layer, α , by the total number of build layers l , and (iii) the total time associated with the amount of material deposited in each layer. Equation (1) summarizes T_{Build} , using a triple Σ operator to express the summation of the time needed to process each voxel in a three-dimensional array representing the discretized build configuration:

$$T_{Build} = T_{Job} + (\alpha \times l) + \sum_{z=1}^z \sum_{y=1}^y \sum_{x=1}^x \left(\beta \times \frac{125\text{mm}^3}{lt} \times \frac{VP_i}{VA_i} \right) \quad (1)$$

The processing of each voxel belonging to part ‘ i ’ is modelled by multiplying a platform specific time increment for deposition (β), essentially expressing the time needed to deposit material corresponding to a single mm^2 of cross-sectional area, by the total number of such increments associated with the $(5 \text{ mm})^3$ voxel. This measure is multiplied by the ratio of the true volume of the part, VP_i (inclusive of supports), and the volume of the voxel approximation, VA_i . In this model, no allowance is made for build preparation and machine cleaning. It is felt that the time spent on these activities is difficult to measure and very much at the discretion of the machine operator. It could be argued that these activities take place during the hours in which the machine is not operating.

The total energy used by the build operation, E_{Build} , is modelled simply by adding the energy consumed to start the system up (E_{Job}) to the time dependent element of energy consumption, which is obtained by multiplying the measured process energy consumption rate $\dot{E}_{Process}$ by the build time estimate T_{Build} :

$$E_{Build} = E_{Job} + (\dot{E}_{Process} \times T_{Build}) \quad (2)$$

The final element of the model is the specification of a cost estimator C_{Build} employing the estimator of build time (T_{Build}) and total energy consumption (E_{Build}). As the product of an activity-based costing model, C_{Build} is obtained by adding the total time-dependent indirect costs, obtained by multiplying an indirect cost rate $\dot{C}_{Indirect}$ by T_{Build} , and adding estimates of direct cost contributions in terms of raw material and energy. The costs incurred for raw materials, of which there are three (see Table 1), are obtained by forming the dot product between a three element vector of used material volume \mathbf{m} and a three element vector of raw material prices \mathbf{p} . Material wastage occurring due to a planarization device built into the print head is accounted for by a uniform waste factor ω . The total energy costs are simply obtained by multiplying the energy price by the consumption estimate E_{Build} . Thus, C_{Build} can be modelled as follows:

$$C_{Build} = (\dot{C}_{Indirect} \times T_{Build}) + \left(\begin{bmatrix} m1 \\ m2 \\ m3 \end{bmatrix} \cdot \begin{bmatrix} p1 \\ p2 \\ p3 \end{bmatrix} \times \omega \right) + (E_{Build} \times ep) \quad (3)$$

Data collection experiment

After specifying the estimators for T_{Build} , E_{Build} and C_{Build} , the next step is to collect empirical data for the Object Connex 260. As observed during previous research (Baumers et al., 2014), the layer-by-layer operating principle usually found in 3D Printing provides an opportunity to investigate whether cross-sectional area impacts the build time per layer.

To facilitate this investigation, a new type of multi-material test part has been designed. It features variation in terms of cross-sectional area and material composition along the Z dimension. The resulting test part, shown in Figure 2, exhibits discrete variation in the two parameters, build material and cross-sectional area, in seven horizontal sections, each with a Z-height of 0.5 mm. By reducing the cross-sectional area of the test part, from 5500 mm² down to 900 mm², as summarized in Table 2, it is possible to investigate if this measure of area correlates with the time needed to process individual layers, hence exploring if the deposited geometry has an effect on build speed.

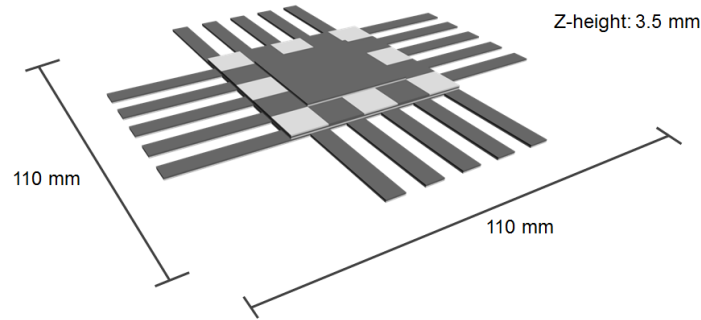


Figure 2: Layer-by-layer design of the test part
Image source: own work

Table 2: Test part characteristics, in 0.5 mm increments of Z-height

| Part section (from top to bottom) | Material | Layer area (mm ²) |
|---|---------------------------------------|-------------------------------|
| Top square (30 × 30 mm) | TangoBlack | 900 |
| Top square (30 × 30 mm) | VeroClear | 900 |
| Middle square (50 × 50 mm) | Mixed (52% VeroClear, 48% TangoBlack) | 2500 |
| Middle square (50 × 50 mm) | TangoBlack | 2500 |
| Middle square (50 × 50 mm) | VeroClear | 2500 |
| Bottom star shape (110 × 110 mm) | TangoBlack | 5500 |
| Bottom star shape (110 × 110 mm) | VeroClear | 5500 |
| Supports (~110 × ~110, height: 1.06 mm) | Support SUP705 | 5500* |

* = Estimate based on the plan view of the test part

To be reflective of full system capacity utilization (Baumers et al., 2013) a total of four multi-material test geometries were included in the data collection experiment, which was run once. The empirical data on build time were extracted from the system's internal log files and process energy consumption was monitored using a Yokogawa CW240 digital multi-purpose power meter, logging actual real power consumption in a 0.1s measurement cycle.

Validation experiment

To validate the model, the build time and energy consumption of the actual machine specification were estimated and then compared to experimental measurements on the real

system. To eliminate the possible effect of capacity underutilization (Baumers et al., 2011), a full build experiment was specified by drawing multi-material test parts from a representative basket of (non-functional) multi-material sample components. This basket, shown in Figure 3, contains a bearing block with embedded structures resembling conductive tracks (a), a belt link component with an internal structure approximating RFID functionality (b), and a small end cap with embedded identification markings (c). This full build experiment was run once.

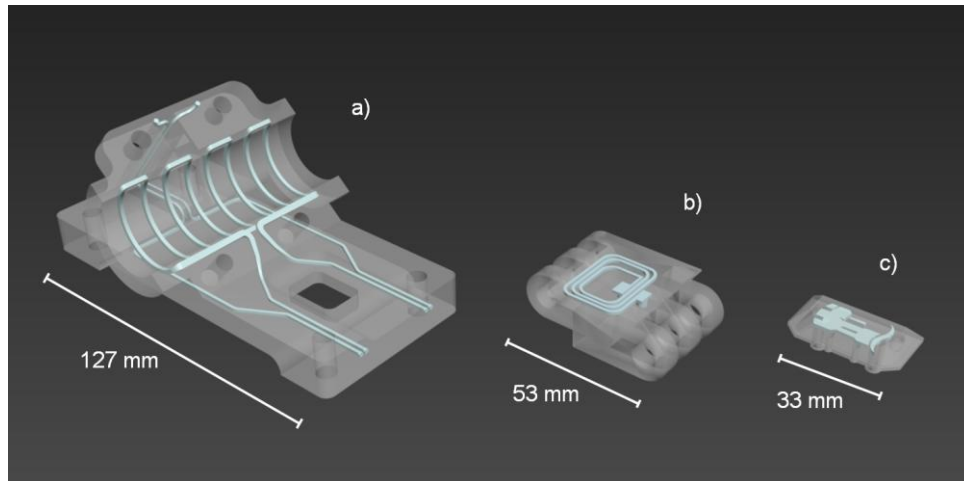


Figure 3: Rendering of multi-material model parts, with embedded structures highlighted

Image source: own work

Results

Data collection results

The data used to construct the build time model were extracted from the internal log files generated by the Objet Connex 260. The data flow into the above specification through the central parameters of the model, α_1 , the fixed time consumption for the deposition of each layer, and β , the time needed to deposit material corresponding to each mm^2 of cross sectional area. The estimates were obtained from an ordinary least squares regression of measured layer deposition time on cross-sectional area ($\alpha_1 = 21.69$, $\beta = 0.0007$). It is noteworthy that the control system's measurements of the layer time during the deposition of the first nine layers of the support structure were inconsistent (ranging from 0 s to 310 s with a mean of 45.78 s). This indicates a control system malfunction and results in a low R^2 measure of the regression (0.048).

In the final model specification, which was chosen to be reflective of higher capacity utilization than the data collection experiments, the parameter α_1 was replaced by a modified parameter α_2 , which was obtained by calculating the mean of the measured layer deposition time of the lower three sections of the multi-material test geometry ($\alpha_2 = 37.25$), thus effectively ignoring the narrowing of the upper sections of the test part (shown in Figure 2).

Included in the information generated through the data collection experiment is a process waste factor ω , which is obtained from the control system's own estimates for waste generated in conjunction with the experiment. Calculated simply by forming the mean of the system's projections of material consumption and waste incurred across three materials, it is estimated at $\omega = 1.76$. Thus, ω indicates that for every kg of material deposited, 0.76 kg of

raw material are discarded as waste. Beyond this, the model constructed for this paper draws on a set of machine and cost parameters from the literature. Table 3 reports the full set of machine and cost parameters used by the model.

Table 3: Set of model parameters used for model specification and data sources

| Variable Group | Variable / parameter | Value | Unit | Data Source |
|----------------|---|--------|-------------------|------------------------------------|
| Build time | Machine start-up (T_{Job}) | 254 | s | - |
| | Fixed time per layer (α_2) | 37.25 | s | - |
| | Deposition time increment (β) | 0.0007 | s/mm ³ | - |
| | Layer thickness (lt) | 30 | μm | Stratasys (2014) |
| Energy | Fixed energy per job (E_{Job}) | 0.10 | MJ | - |
| | Energy consumption rate ($\dot{E}_{Process}$) | 533.1 | J/s | - |
| Cost | Indirect cost rate ($\dot{C}_{Indirect}$) | 26.01 | \$/h* | Adapted from Baumers et al. (2013) |
| | Material cost, VeroClear (p_1) | 419.90 | \$/kg* | Sys Ltd. (2014) |
| | Material cost, TangoBlack (p_2) | 419.40 | \$/kg* | Sys Ltd. (2014) |
| | Material cost, Support (p_3) | 142.02 | \$/kg* | Sys Ltd. (2014) |
| | Waste factor (ω) | 1.76 | - | - |
| | Energy price (ep) | 0.031 | \$/MJ* | Adapted from Baumers et al. (2013) |

* = estimated using a \$/£ exchange rate of 1.71

Validation of model performance

Figure 4 shows the full build experiment, as specified by the build volume packing algorithm. The full build contains 3 bearing block components, 6 belt links, and 15 end caps. Of the available 2500 build volume floor voxels, sized (5 mm)³, the algorithm has filled 2151. The resulting utilization level (86%) indicates an acceptable packing performance when compared to other implementations of this functionality (Baumers et al., 2013).

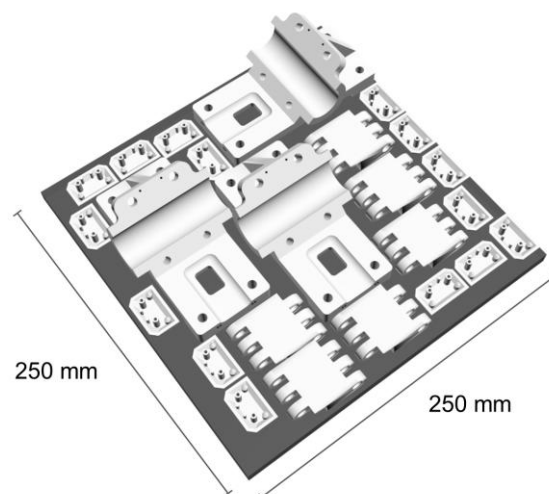


Figure 4: Full build packing specification on Objet Connex 260

Image source: own work

Table 4 compares the model estimates to the experimental build time and process energy consumption measurements and reports estimation errors. These can be compared to corresponding errors from the literature (Ruffo et al., 2006; Campbell et al., 2008; Munguia, 2009; Wilson, 2006; Di Angelo and Di Stefano, 2011; Baumers et al., 2013), ranging from 1.03% (Baumers et al., 2013) to 22.68% (Wilson, 2006). The reported estimator performance suggests a reasonable degree of accuracy.

Table 4: Estimator accuracy against experimental data

| | Model estimate | Validation experiment | Error |
|--|----------------|-----------------------|--------|
| Number of parts in the build | 24 | 24 | - |
| Total build time (T_{Build}) | 1406.26 min | 1206.85 min | 14.18% |
| Total energy consumption (E_{Build}) | 44.95 MJ | 37.79 MJ | 18.93% |

Using the model

Once the combined model has been assembled and tested, individual aspects of this model can be modified in a “ceteris paribus” manner (keeping everything else constant) to explore how individual upgrades to the investigated AM platform affect the overall measures of machine productivity, process energy consumption and financial cost. It is useful to analyze the effects in terms of absolute deposition rate (cm^3/h), specific energy consumption (MJ/cm^3) and specific cost ($\$/\text{cm}^3$) and also in terms of relative percentage improvements over the platform’s performance in its baseline configuration.

In total, 12 machine characteristics were upgraded, one at a time, requiring the implementation to be adjusted and re-executed. The improvements analyzed include: (i) aspects of machine architecture, such as build volume size and layer thickness, (ii) machine performance characteristics, such as deposition speed and machine lifespan, and (iii) reduced input prices for raw materials and energy. The idea guiding this analysis is to explore the effect of a 20% improvement in each characteristic. Table 5 reports the upgraded platform characteristics and the outcomes of the simulation using the detailed process model developed in this paper.

Table 5: Machine upgrades and effects on the Objet Connex 260 process model

| | Absolute effect | | | Effect relative to the unmodified process model | | |
|--|--------------------|--------------------|--------------------|---|--------|--------|
| | Build rate | Energy | Cost | Build rate | Energy | Cost |
| | cm ³ /h | MJ/cm ³ | \$/cm ³ | % | % | % |
| Unmodified process model | 17.75 | 0.11 | 2.56 | - | | |
| Process energy consumption reduction (20%) | 17.75 | 0.09 | 2.56 | - | -20.00 | -0.03 |
| Uniform build volume scale-up (20% in X, Y, and Z dimensions) | 25.01 | 0.08 | 2.14 | 29.03 | -29.03 | -16.63 |
| Layer thickness increase (20% to 36 μ m) | 21.28 | 0.09 | 2.32 | 16.60 | -16.61 | -9.51 |
| Head movement / deposition speed increase (20%) | 22.17 | 0.09 | 2.27 | 19.94 | -19.96 | -11.42 |
| Warm-up time decrease (20%) | 17.76 | 0.11 | 2.56 | 0.06 | - | -0.03 |
| Waste material decrease (20%, $\omega = 1.61$) | 17.75 | 0.11 | 2.47 | - | - | -3.75 |
| Machine purchase cost decrease (20%) | 17.75 | 0.11 | 2.49 | - | - | -2.72 |
| Annual operating time increase (20%, to 6000 h) | 17.75 | 0.11 | 2.44 | - | - | -4.92 |
| Primary (VeroClear) material cost decrease (20%, to 335.92 \$/kg) | 17.75 | 0.11 | 2.39 | - | - | -6.70 |
| Secondary (TangoBlack) material cost decrease (20%, to 335.53 \$/kg) | 17.75 | 0.11 | 2.56 | - | - | -0.10 |
| Energy cost decrease (20%, to 0.025 \$/MJ) | 17.75 | 0.11 | 2.56 | - | - | -0.03 |
| Machine lifespan (depreciation period) increase (20%, to 9.6 years) | 17.75 | 0.11 | 2.51 | - | - | -2.28 |

For a graphical illustration, Figure 6 reports the relative impacts in bar chart form. It is apparent that build volume size increase (in the X, Y and Z dimensions), layer thickness increase and faster deposition speed have significant cost reducing effects (ranging from -16.63% to -11.42%). Other improvements, such as energy consumption reduction, faster machine warm up, and reduction of the price of the secondary build material (of which only approximately 6.24 cm³ were deposited), and a reduction of the energy price have only a negligible effect on the platform's cost performance.

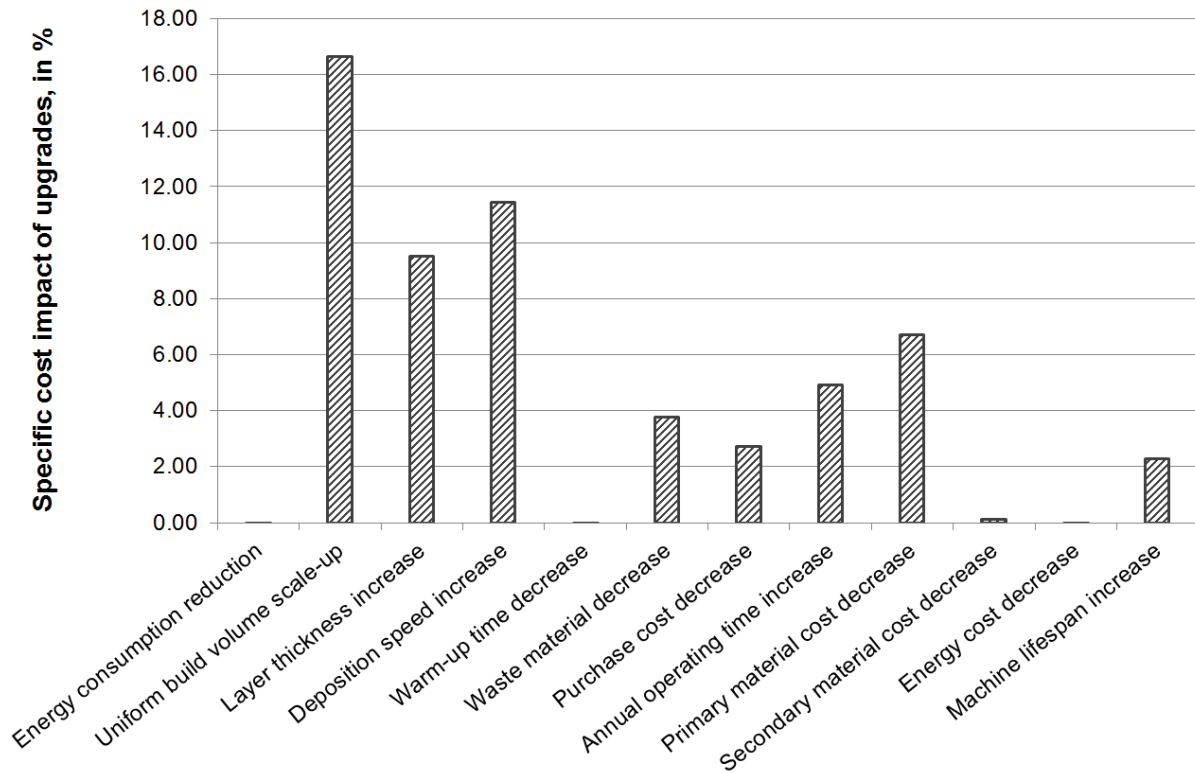


Figure 5: Relative effect on specific cost of system improvements

Image source: own work

Discussion

The constructed model indicates that AM platforms based on material jetting technology appear to benefit significantly in terms of build rate and process cost if improvements towards higher machine capacity and throughput are made. This scalability aspect is noted in the literature (Gibson et al., 2010) and is evidenced through experimental high volume manufacturing platforms based on direct material jetting (TNO, 2011; Project Ara, 2014).

The presented model also suggests that scaling up the dimensions of the build volume produces a greater benefit in all three assessed categories (time, energy and cost) than a corresponding increase in the deposition speed. This, possibly counterintuitive, result occurs due to the specification of the build size increase as a 20% increase in the dimensions of the build volume, which does not equate to a 20% increase in the build volume cuboid. Rather, it equates to an increase of approximately 73% in volume (according to the square-cube law). While not part of this investigation, it is safe to assume that a 20% increase in the volume of the build cuboid (from approximately 12,500 cm³ to 15,000 cm³) would have had a far smaller impact on platform performance.

The usefulness of current material jetting systems for manufacturing applications is limited by the range of build materials available (Diginova, 2014). Commercial direct material jetting platforms are restricted to photopolymers, such as the materials investigated in this research, and waxes (Gibson et al., 2010). Such materials can have non-standard properties that constrain their functionality, such as poor mechanical properties, material

degradation if exposed to UV radiation, and toxicity. Moreover, as demonstrated in Table 3, the materials available for the Objet Connex 260 are currently very expensive, with prices ranging from 142.02 to 419.40 \$/kg. Unsurprisingly, the overall cost performance of the investigated system is especially sensitive to the cost of the primary structural material (VeroClear in this case). This suggests that acceptable raw material prices, in particular for the bulk structural material, will be critical for the value proposition of material jetting processes in manufacturing.

The general purpose framework adapted by this paper has originally been specified to be applicable to all variants of AM, with an emphasis on powder bed fusion systems (see Baumann et al., 2013). This analysis shows that the differing operating principle of material jetting technology makes the application of such a general model difficult. The reason for this lies in the fact that jetting processes do not necessarily exhibit a relationship between deposition volume / geometry and build time. Such a relationship has been observed in filament extrusion systems and, to a limited extent, in powder bed fusion systems (Baumann et al., 2011). This is because material jetting systems operate through a succession of discrete print head movements in the X / Y plane, effectively depositing material in a frontier that moves in passes across the available build space. On the Objet Connex 260, it does not appear to be of relevance for print head movement speed if material is actually deposited or not.

Complicating matters, the data collection experiment has shown that the print head will not exhaust its full movement range (both in the X and Y dimensions) if the build specification does not demand it. Therefore, a relationship between the amount of material deposited and build time must be expected. Deposition in terms of print head passes can make the time needed to deposit additional material very lumpy. Effectively, the time required to deposit additional geometry depends on whether extra Y-passes, or even Z-layers, are needed. This difficulty results in an inaccurate specification using the original parameter α_1 , necessitating its replacement by α_2 . In planned further research, which will result in a journal submission, the model proposed in this paper will be re-specified to decrease the observed estimation errors, which are currently ranging from 14.18% to 18.93%.

It is noteworthy that this paper assesses a process depositing multiple materials through a multi-print head assembly moving in unison, referred to as a “print block”. This configuration implies that the process regime for the two build materials and the auxiliary support material are very similar (if not identical). In particular, this allows the first two elements of the process model (T_{Build} and E_{Build}) to be collapsed into the single material case. Clearly, this is not possible where multi-material AM is based on entirely dissimilar deposition processes such as those described by Espalin et al. (2014) or Vogeler et al. (2013), for example combining filament deposition and aerosol jetting processes. Similar considerations apply to the specification of a uniform waste factor ω applying to all deposited materials. This specification may not be appropriate for platforms with more dissimilar sub-processes. This paper recommends that work should be undertaken to establish a taxonomy of multi-material AM processes to provide structure to investigations of their implementation.

Conclusions

This paper has demonstrated that a combined model of build time, process energy consumption and financial cost for a multi-material AM system can serve as a very efficient

avenue for initial thought experiments on how such systems could be advanced in the future. Effectively, it shows how such a model can be used to gain an understanding of effects of specific process upgrades. In terms of modelling results, this paper suggests that increasing system productivity, build volume dimensions and the layer thickness would have a strong positive effect on process performance in terms of productivity, energy efficiency and financial cost.

The importance of correctly measuring and plausibly anticipating the cost performance of novel process variants should not be underestimated. The net benefit, or value, of any technology can be investigated by analyzing the difference between the costs associated with it and its gross benefits. This implies that the potential for value creation residing within processes is inextricably bound up with their cost performance. In the near future, such patterns will be of particular interest to the proponents of multi-material AM systems which are expected to enable manufacturers and designers to efficiently create high value embedded functionality *en masse*. Modelling the costs of such multi-material systems credibly and showing that they can be reduced by incremental technology improvement brings the manufacturing industry one step closer to implementing this exciting and ground-breaking new technology.

Acknowledgements

The authors acknowledge the support and technical expertise provided over the course of this research by the 3DPRG's technical staff Joe White, Mark East and Mark Hardy.

References

1. Alexander, P., Allen, S., and Dutta, D., 1998. Part orientation and build cost determination in layered manufacturing, *Computer-Aided Design*, 30 (5), pp. 343-356.
2. ASTM, 2012. "ASTM F2792 - 12e1 Standard Terminology for Additive Manufacturing Technologies," www.astm.org/Standards/F2792.htm.
3. Atrill, P., and McLaney, E., 1999. *Management Accounting for Decision Makers*, 2nd ed. London: Prentice Hall Europe.
4. Baumers, M., Tuck, C., Wildman, R., Ashcroft, I., Rosamond, R., and Hague, R., 2013. Transparency built-in: energy consumption and cost estimation for Additive Manufacturing, *Journal of Industrial Ecology*, 17(3) (2013) pp.418-431.
5. Baumers, M., Tuck, C., Wildman, R., Ashcroft, I., and Hague, R., 2011. Energy inputs to additive manufacturing: does capacity utilization matter?, *Proceedings of the Solid Freeform Fabrication (SFF) Symposium 2011*. The University of Texas at Austin.
6. Baumers, M., Tuck, C., Wildman, R., Ashcroft, I., and Hague, R., 2014, Is there a relationship between product shape complexity and process energy consumption in Additive Manufacturing?, *Sustainable Design and Manufacturing 2014*, 28-30 April.

7. Bourell, D. L., Beaman, J. J., Leu, M. C., Rosen, D. W., 2009. A Brief history of additive Manufacturing and the 2009 Roadmap for Additive Manufacturing: Looking Back and Looking Ahead, RapidTech 2009: US-Turkey Workshop on Rapid technologies, Istanbul.
8. Byun, H., Lee, K. H., 2006. Determination of the optimal build direction for different rapid prototyping processes using multi-criterion decision making, *Robotics and Computer-Integrated Manufacturing*, 22 (1), pp.69-80.
9. Cotteleer, M., and Joyce, J., 2014. 3D opportunity: Additive manufacturing paths to performance, innovation, and growth [Online] Deloitte, <http://dupress.com/articles/dr14-3d-opportunity> [Accessed: 12.06.2014].
10. Campbell, I., Combrinck, J., De Beer, D., and Barnard, L., 2008. Stereolithography build time estimation based on volumetric calculations, *Rapid Prototyping Journal*, 14 (5), pp. 271-279.
11. Di Angelo, L., Di Stefano, P., 2011. A neural network-based build time estimator for layer manufactured objects. *The International Journal of Advanced Manufacturing Technology*, 57 (1) pp.215-224.
12. Diginova – Innovation for Digital Fabrication, 2014. Roadmap for Digital Fabrication [Online], available from: http://www.diginova-eu.org/content/dam/diginova/en/documents/Digital_Fabrication_eBook.pdf [Accessed: 17.05.2014]
13. Espalin, D., Muse, D. W., Macdonald, E., Wicker, R. B., 2014. 3D Printing multifunctionality: structures with electronics, *International Journal of Advanced Manufacturing Technology*, 72(1), pp.963-978.
14. Gibson, I., Rosen, D., W., Stucker, B., 2010, *Additive Manufacturing Technology – Rapid Prototyping to Direct Digital Manufacturing*. Springer, New York.
15. Hur, S., Choi, K., Lee, S., Chang, P., 2001. Determination of fabricating orientation and packing in SLS process, *Journal of Materials Processing Technology*, 112 (1), pp. 236-243.
16. Ikonen, I., Biles, W. E., Kumar, A., Ragade, R. K., Wissel, J. C., 1997. A Genetic Algorithm for Packing Three-Dimensional Non-Convex Objects Having Cavities and Holes, *Proceedings of the 7th International FAIM Conference*, Middlesborough, United Kingdom.
17. Lipson, H., 2012, “Frontiers in Additive Manufacturing,” *The BRIDGE – National Academy of Engineering*, 41, pp. 5-12.
18. Melchels, F. P., 2012. Celebrating three decades of stereolithography, *Virtual and Physical Prototyping*, 7(3), pp173-175.
19. Mognol, P., Lopicart, D., and Perry, N., 2006. Rapid prototyping: energy and environment in the spotlight, *Rapid Prototyping Journal*, 12(1), pp. 26-34.
20. Munguia, F. J., 2009. RMADS: Development of a concurrent Rapid Manufacturing Advice System, Ph.D. thesis, Universitat Politecnica de Catalunya, Barcelona, Spain.
21. Nyaluke, A., Nasser, B., Leep, H. R., Parsaei, H. R., 1996. Rapid prototyping work space optimization, *Computers ind. Engng.* 31 (1/2), pp. 103-106.

22. Project Ara, 2014. Corporate Website [Online]. Available from: <http://www.projectara.com> [Accessed: 01.07.2014].
23. Ruffo, M., Tuck, C., and Hague, R., 2006. Cost estimation for rapid manufacturing – laser sintering production for low to medium volumes, *Proceedings of IMech E Part B: Journal of Engineering Manufacture*, 220 (9), pp.1417-1427.
24. Ruffo, M., and Hague, R., 2007. Cost estimation for rapid manufacturing – simultaneous production of mixed components using laser sintering, *Proceedings of IMech E Part B: Journal of Engineering Manufacture*, 221(11), pp.1585-1591.
25. Shellabear, M., and Nyrhilä, O., 2004. DMLS – Development history and state of the art, LANE 2004 conference, Sept. 21-24, Erlangen, Germany.
26. Stratasys Inc., 2014. Corporate Website [Online]. Available from: www.stratasys.com [Accessed: 01.07.2014].
27. Sys Ltd., 2014. Corporate Website [Online]. Available from: www.sys-uk.com [Accessed: 12.06.2014].
28. TNO, 2011. Fast and Flexible Production [Online]. Available from: <https://www.tno.nl/downloads/LR%20Leaflet%20Fast%20and%20Flexible%20production21.pdf> [Accessed: 10.06.2014].
29. Tuck, C. J., Hague, R. J. M., Ruffo, M., Ransley, M., and Adams, P., 2008. Rapid Manufacturing facilitated customization, *International Journal of Computer Integrated Manufacturing*, 21(3), pp.245-258.
30. Vogeler, F., Verheecke, W., Voet, A., Valkenaers, H., 2013. An Initial Study of Aerosol Jet Printed Interconnections on Extrusion-Based 3D-Printed Substrates, *Journal of Mechanical Engineering* 59(11), pp.689-696.
31. Wilson, J. O., 2006. Selection for rapid manufacturing under epistemic uncertainty, Master's thesis. Georgia Institute of Technology, Atlanta, USA.
32. Wodziak, J. R., Fadel, G. M., Kirschman, C., 1994. A genetic algorithm for optimizing multiple part placement to reduce build time, *Proceedings of the Fifth International Conference on Rapid Prototyping*, Dayton, USA, pp. 201-210.
33. Wohlers, T., ed., 2012. *Wohlers Report 2012*. Fort Collins: Wohlers Associates, Inc.